Chromomycin A_2 potently inhibits glucose-stimulated insulin secretion from pancreatic beta cells.

Michael A Kalwat*[1], In Hyun Hwang[2], Jocelyn Macho[3], Magdalena G Grzemska[1], Jonathan Z Yang[1], Kathleen McGlynn[1], John B MacMillan[3], Melanie H Cobb*[1].

[1]Department of Pharmacology, UT Southwestern Medical Center, Dallas, TX. [2]Department of Pharmacy, Woosuk University, South Korea. [3]Department of Chemistry & Biochemistry, UC Santa Cruz, Santa Cruz, CA

*Correspondence:

Dr. Michael A Kalwat, Department of Pharmacology, UT Southwestern Medical Center, Dallas, TX 75235, USA; Michael.Kalwat@utsouthwestern.edu

Dr. Melanie H Cobb, Department of Pharmacology, UT Southwestern Medical Center, Dallas, TX 75235, USA; Melanie.Cobb@utsouthwestern.edu

ABSTRACT (298 words)

Compounds that enhance or inhibit insulin secretion could become therapeutics as well as lead to the identification of requisite β cell regulatory pathways and increase our understanding of pancreatic islet function. Toward this goal, we previously generated an insulin-linked luciferase that is co-secreted with insulin in MIN6 β cells. With this assay we completed a high-throughput natural product screen for chronic effects on glucose-stimulated insulin secretion. Using a distributive phenotypic analysis approach we

identified that one of the top natural product hits, chromomycin A2 (CMA2), potently inhibited insulin secretion (EC_{50}=11.8 nM) through at least three mechanisms: disruption of Wnt signaling, interfering with β cell gene expression, and suppression of triggering calcium influx. Chronic treatment with CMA2 largely ablated glucose-stimulated insulin secretion even post-washout, but did not inhibit glucose-stimulated generation of ATP, Ca^{2+} influx, or ERK1/2 activation. However, experiments using the K_{ATP} channel opener diazoxide uncovered defects in the triggering Ca^{2+} influx which may contribute to the suppressed secretory response. Using the FUSION bioinformatic database, we found that the phenotypic effects of CMA2 clustered with a number of Wnt/GSK3β pathway-related genes. Consistently, CMA2 decreased GSK3β phosphorylation and suppressed activation of a β-catenin activity reporter. CMA2 and a related natural product mithramycin are described to have DNA-interaction properties, possibly abrogating transcription factor binding to critical β cell gene promoters. We observed that CMA2, but not mithramycin, suppressed expression of PDX1 and UCN3. Neither expression of INSI/II or insulin content was affected. We conclude that chronic treatment with CMA2 treatment results in the disruption of signaling pathways and expression of genes that support β cell function that both support Ca^{2+} influx and are required downstream, independent of insulin abundance. Future applications of CMA2 and similar aureolic acid analogs for disease therapies should consider the potential impacts on pancreatic islet function.

INTRODUCTION

Insulin secretion from β cells is one of the most important functions of the pancreatic islet. Type 1 and type 2 diabetes combined afflict 9.4% of Americans (1) and result from the autoimmune destruction of β cells, or defects in insulin secretion and action, respectively. Insulin secretagogues, potentiators and replacement are used therapeutically, however insulin hypersecretion also occurs in type 2 diabetes and other disorders such as persistent hyperinsulinemic hypoglycemia of infancy and polycystic ovary syndrome (2-4). Accordingly, inhibition of insulin secretion has been considered in the past as a potential therapeutic avenue (5). Much is known about the stimulus-secretion coupling of glucose-stimulated insulin secretion; however, less is understood about the glucose-mediated metabolic amplification pathway in β cells which can account for half of the insulin secretion response (6,7). In particular, the signaling pathways and transcriptional outputs that are chronically required for β cell function are not completely understood. Further development of knowledge and tools pertaining to these aspects of the β cell is required to uncover new directions for research that eventually lead to disease therapies.

Marine natural products are a rich resource for potential new chemical tools and therapies. Screening of a unique custom library of natural compounds assembled at UT Southwestern has been utilized to discover new leads for chemotherapies (8-11), inhibitors of endocytosis (12), antibiotics (13), and modulators of pancreatic beta cell function (14). Through our recent screening efforts (14), we discovered that the natural product chromomycin A_2 (CMA2) is a potent inhibitor of insulin secretion. CMA2 is part of a family of glycosylated aromatic polyketides called aureolic acids. This family

includes a variety of chromomycins, olivomycins, chromocyclomycin, duhramycin A, as well as the founding member mithramycin (MTM) (15). This class of compounds is known to interact with the minor groove of DNA in a non-intercalative way with a preference for GC-rich regions (16). This mechanism is more subtle and distinct from other transcription inhibitors like actinomycin D which binds DNA at the transcription elongation complex (17) or α-amanatin which directly inhibits RNA polymerase II (18). Based on their known activities, aureolic acids have been pursued as anti-cancer chemotherapies. For example, these compounds have been implicated as anti-tumor agents (15,19), inhibitors of Wnt signaling (20) and DNA gyrase (21), as well as autophagy inducers (22,23), although the specific genes and pathways implicated in the mechanism of action of CMA2 and MTM are only just being fleshed out.

Over the past five years a unique bioinformatic tool called Functional Signature Ontology (FUSION) has been continually developed. FUSION bridges the phenotypic impact of natural and synthetic chemicals to clusters of genes that are mechanistically implicated (9-11,24,25). Here we applied FUSION to CMA2 and found that suppression of genes connected to Wnt signaling and Glycogen Synthase Kinase 3β (GSK3β) cluster with CMA2. The requirements for the Wnt pathway in β cell development and function are clear (26-29), therefore new chemical tools to interrogate this pathway are of immediate relevance to the field of diabetes and islet biology.

RESULTS

Identification of Chromomycin A_2 as an insulin secretion inhibitor

We previously performed a natural product screen using specialized MIN6 β cells containing an insulin promoter-driven Gaussia luciferase-linked insulin transgene (14). Cells were treated chronically (24 h) with compounds, preincubated in KRBH in the absence of compounds, and then stimulated. This strategy allowed us to probe a specific pharmacological space where hit compounds must have long-lasting impacts or effects that are essentially irreversible within the preincubation and stimulation periods. In the screen we stimulated the cells using the diazoxide paradigm to drive both the triggering and metabolic amplifying pathways of insulin secretion (30,31) to provide a platform to later assign the actions of hit compounds to triggering and/or amplification and give maximal dynamic range in the assay. From the screen, we selected natural product fractions that appeared non-toxic after an overnight treatment but still potently inhibited glucose-stimulated insulin secretion. Among the top hits was fraction SNB-022-1 derived from *Streptomyces anulatus*. In rescreening we found this fraction retained the expected inhibitory activity (**Fig 1A**). Further fractionation, high resolution mass spectrometry analyses and NMR analyses showed the major component of the fraction to be chromomycin A_2 (CMA2) (**Fig S1A,B**). We determined the EC_{50} of CMA2 in our reporter assay to be 11.8 nM (**Fig 1B**).

We began to determine the mechanism of CMA2-mediated inhibition of insulin secretion, by first testing whether a short (2 h) treatment with CMA2 was sufficient for inhibitory activity, as opposed to the overnight chronic treatment. Short-term treatment with CMA2 did not prevent glucose-stimulated secretion in our reporter β cells (**Fig 1C**),

suggesting against a rapid mechanism of action. We confirmed the effects of overnight treatment with CMA2 in human islets, where it suppressed glucose-stimulated insulin secretion in a static culture assay (**Fig 1D**). We then measured calcium influx in normal MIN6 cells pre-treated with CMA2. In response to glucose, calcium influx was not different between vehicle- and CMA2-treated cells (**Fig 1E**), suggesting the dramatic ablation of glucose-stimulated insulin secretion was not due primarily to a defect in glucose-stimulated calcium influx. However, we also tested calcium influx under the diazoxide paradigm and found that was indeed a suppression of the triggering calcium influx (**Fig 1F**). Diazoxide and KCl clamped the calcium levels as expected; glucose stimulation did not cause any additional changes in intracellular calcium levels (**Fig 1F**, green vs orange and purple vs black). To address whether well-known glucose-mediated β cell signaling pathways are disrupted by CMA2, we tested glucose-induced ERK1/2 MAP kinase (32-35) and ribosomal protein S6 phosphorylation (36,37). MIN6 cells were treated overnight with DMSO or CMA2 and the following day preincubated in KRBH containing either DMSO or CMA2 to result in cells treated acutely (2 h in CMA2-KRBH), chronically (24 h + 2 h in CMA2-KRBH), or chronically with a washout (24 h + 2 h in DMSO-KRBH). After the 2 h KRBH incubation, the cells were stimulated with glucose which activated ERK1/2 phosphorylation by 5 min (**Fig 1G**). Chronic CMA2 treatment suppressed ERK1/2 activation at the 5 min time point, while by 30 min all CMA2 treatments had suppressed glucose-stimulated ERK1/2 phosphorylation with respect the 0 min time point (**Fig 1G, upper right**). With respect to S6 phosphorylation, in control and acute CMA2-treated cells, pS235/6-S6 was induced by 30 min, whereas both chronic CMA2 treatments blunted this event (**Fig 1G, bottom right**).

Chromomycin A_2 disrupts Wnt/GSK3β pathway signaling in MIN6 β cells.

To aid in discerning the signaling pathways impacted by CMA2, we used a database developed on-campus called FUSION (10,24). The FUSION database was generated by measuring a genetic perturbation signature in response to whole genome siRNA, synthetic and natural product screening. The resulting network allowed us to query what genes may be involved in the actions of CMA2. Through FUSION, we found that CMA2-containing natural product fractions clustered with a small set of genes. Using the online tool Enrichr (http://amp.pharm.mssm.edu/Enrichr/) (38), we determined this cluster contained Wnt/GSK3β-linked genes (**Fig 2A**). In agreement with these findings, chromomycin compounds were previously linked to Wnt pathway inhibitory activity (20). When GSK3β is not phosphorylated at serine 9, it is active and can phosphorylate β-catenin targeting it for proteasomal degradation. Wnt signaling or small molecule inhibitors of GSK3β lead to accumulation of β-catenin, thereby increasing expression of Wnt-responsive genes (26). We observed similar CMA2-induced inhibition in the Super TOPFlash assay in HEK293 cells, even in the face of a potent inhibitor of GSK3β, CHIR99021, which potently activates reporter expression (**Fig 2B**). To assess the general impact of CMA2 on induced transcription in divergent reporter assays, we employed cell line-based reporters of TGFβ/Smad and TNFα/NFkB activity. We found that in the case of Smad activation by TGFβ (**Fig S2A**) and NFkB activation by TNFα (**Fig S2B**), 1-10 nM CMA2 had little effect or a slight potentiating effect, respectively. 100 nM CMA2 completely suppressed the response in both assays. These data suggest that at high doses, CMA2 has general inhibitory effects in transcriptional reporter

assays, likely due to its DNA binding properties, similar to its related natural product mithramycin. However, because CMA2 inhibits glucose-stimulated insulin secretion with an EC_{50} on the order of ~10 nM, there are likely nuanced mechanisms apart from simple transcriptional inhibition.

Chronic CMA2 treatment of MIN6 cells also resulted in suppressed GSK3β serine 9 phosphorylation and increased degradation of β-catenin (**Fig 2C**). We also observed that another small molecule Wnt signaling inhibitor and GSK3β activator, pyrvinium, led to dramatic suppression of glucose-stimulated insulin secretion in our reporter assay (**Fig 2D**), in agreement with recently published findings on the effects of this compound in islet β cells (27).

Chromomycin A_2 suppresses β cell gene expression

Given what is known about mithramycin-DNA binding activity (16), mithramycin's effect on gene expression in glioblastoma models (19), and the structural similarities between CMA2 and mithramycin (**Fig S1B**), we tested CMA2 and mithramycin side-by-side in our insulin secretion reporter assays. Interestingly, CMA2 was about 50 times more potent than mithramycin at inhibiting glucose-stimulated secretion after overnight incubation (**Fig 3A**). We regularly assess cell viability after secretion experiments using the Cell Titer Glo assay, which measures relative ATP amounts indirectly through a luciferase assay. Interestingly, CMA2-treated cells have an elevated Cell Titer Glo signal while mithramycin-treated cells did not (**Fig 3B**).

Aureolic acid compounds are known to impact transcription, therefore we hypothesized that CMA2 may exert some of its effects on β cell function by suppressing the expression of critical genes. To assess the effects on gene expression we treated MIN6 cells with CMA2 or mithramycin for overnight and extracted RNA for RT-qPCR analysis. CMA2, but not mithramycin, suppressed expression of an important β cell transcription factor, PDX1, at as low as 10 nM (**Fig 3C**). Expression of Urocortin 3 (UCN3), a marker of β cell maturation and paracrine regulation of somatostatin secretion (39,40), was also suppressed but only at 100 nM (**Fig 3C**). Neither INSI/II expression (**Fig 3C**) or insulin content (**Fig S2C**) were affected by CMA2 treatment. As a result of the suppressed gene expression induced by CMA2, a longer-term 72 h treatment results in reduced cell growth/viability as determined by Cell Titer Glo (**Fig S2D**) as well as cell number determined by nuclei counting (**Fig S2E**).

Discussion

Natural products are a useful source of biologically active compounds that may enhance our understanding of β cell function. Through our recent screening efforts we discovered that CMA2 potently inhibits insulin secretion after overnight exposure. In all of the experiments where cells were treated chronically overnight with CMA2, the media and compound were washed off with KRBH before the preincubation and stimulation. This suggests a long-lasting impact of CMA2, perhaps either through transcriptional or protein stability effects. Because CMA2 pre-treatment almost completely blocked secretion in both triggering and amplifying stimulation conditions (**Fig 3A**), we

surmise that the minor reduction in KCl-stimulated calcium influx is unlikely to account for such a dramatic inhibition of secretion (**Fig 1E)**.

We chose to investigate whether the structurally similar (**Fig S1A**) CMA2 relative mithramycin had similar effects, but surprisingly as much as 50 times more mithramycin was required to have the same impact on secretion as 10 nM CMA2. 500 nM mithramycin also did not impact the cells relative ATP concentrations like CMA2, suggesting other mechanistic differences, perhaps at the transcriptional level, in the actions of these two products. Mithramycin was suggested to have tumor selective properties, inhibiting the function a transcriptional trifecta (Sox2, Zeb1, Olig2) to inhibit growth of glioblastoma (19). Given the recent work on mithramycin and less toxic isoforms (19,41), and the high similarity between the mithramycin and CMA2 structures suggests that modified forms of CMA2 may prove useful as therapeutics for different cancers or as chemical probes for research. Over 30 years ago the differences in potency of the aureolic acid family compounds, including mithramycin and CMA2, were suggested to be a result of differential uptake of the compounds into mammalian cells (42). While the mechanistic explanation for the differences between CMA2 and MTM in β cells are unclear, it is possible that in our assays β cells are more sensitive to CMA2 compared to mithramycin due to this differential uptake. However, in glioblastoma models 50 nM mithramycin showed substantial effects on gene expression (19), suggesting 50-100 nM mithramycin is more than sufficient to elicit effects in mammalian cells.

CMA2 at higher doses for longer durations of treatment also exhibited some cytotoxic or cytostatic effects. This is likely due to multiple factors, including inhibition of transcription and blunting of pro-survival β-catenin activity. Additionally, CMA2 was identified to inhibit DNA gyrase *in vitro* at concentrations of above 50 nM (21); however its Wnt pathway inhibitory activity is observed in cells at doses below 5 nM, suggesting dose-dependent target selectivity. This is in-line with our observations of an 11.8 nM EC50 of CMA2 for inhibition of glucose-stimulated insulin secretion and the ability of 10 nM CMA2 to suppress CHIR-induced β-catenin activity.

The uses of these natural products in applications such as chemotherapy warrant consideration of side-effects on β cells or other sensitive tissues. At the same time, identifying targetable pathways to suppress insulin secretion is also a potentially valuable therapeutic approach for diseases such as polycystic ovary syndrome and persistent hyperinsulinemic hypoglycemia of infancy. In some cases these disorders are treatable, but there are many individuals who are not responsive to therapy (43). Insulin secretion inhibitors such as diazoxide, in conjunction with exogenous insulin therapy, have also been used to 'rest' β cells, thereby prolonging endogenous functional β cell mass (44,45), as well as preserve isolated human islet function prior to transplant (46). Given the potential for aureolic acids to modulate the expression of a wide swath of the transcriptome, future studies will require in-depth gene expression analysis to determine the β cell-specific genes which are disrupted in response to CMA2. Discovery of such genes or pathways could provide in-roads into pharmacologically stabilizing β cell function in a variety of disease settings.

Materials and Methods:

Antibodies and Reagents – Chromomycin A2 was purified from extracts of Streptomyces anulatus as described below or purchased (Santa Cruz). Mithramycin was generously provided by Ralf Kittler (UTSW). Antibodies, their dilutions for immunoblotting, and their source information are listed in **Table S1**. All other reagents were obtained through Fisher unless otherwise stated.

Human islet culture and treatments – Human islets were obtained through the Integrated Islet Distribution Program (IIDP). Donor information is provided in **Table S1**. Upon receipt, human islets were cultured in CMRL-1066 containing 10% fetal bovine serum, 100 U/ml penicillin and 100 µg/ml streptomycin. For static culture insulin secretion experiments human islets were hand-picked under a dissection microscope equipped with a green Kodak Wratten #58 filter (47) and placed into low-binding 1.5ml tubes with ~50 islets per tube. Islets were washed twice with Krebs-Ringer Bicarbonate Hepes buffer (KRBH) (134 mM NaCl, 4.8 mM KCl, 1 mM $CaCl_2$, 1.2 mM $MgSO_4$, 1.2 mM KH_2PO_4, 5 mM $NaHCO_3$, 10 mM HEPES pH 7.4, 0.1% BSA) and preincubated in KRBH supplemented with 2 mM glucose for 1 h before switching to KRBH containing either 2 or 16 mM glucose for 1 h. Supernatents were collected, centrifuged at 10,000 x g for 5 min and transferred to fresh tubes for storage at -80°C. Total insulin content was extracted by acid-ethanol overnight at -80°C and was neutralized with an equal volume of 1M Tris pH 7.4 prior to assay.

Cell culture and treatments – MIN6 β cells were cultured in Dulbecco's modified Eagle's medium (which contains 25 mM glucose), supplemented with 15% fetal bovine

serum, 100 units/ml penicillin, 100 µg/ml streptomycin, 292 µg/ml L-glutamine, and 50 µM β-mercaptoethanol as described previously (48). MIN6 cells in 12 well dishes were transfected with Lipofectamine 2000 (for plasmids) (Life Technologies, Inc) according to the manufacturer's instructions and cultured 48 h before use in experiments. Prior to stimulation, MIN6 cells were washed twice with and incubated for 2 h in freshly prepared modified Krebs-Ringer bicarbonate buffer (MKRBB: 5 mM KCl, 120 mM NaCl, 15 mM HEPES, pH 7.4, 24 mM NaHCO3, 1 mM MgCl2, 2 mM CaCl2, and 1 mg/ml radioimmunoassay-grade BSA). Cells were lysed in 25 mM HEPES, pH 7.4, 1% Nonidet P-40, 10% glycerol, 50 mM sodium fluoride, 10 mM sodium pyrophosphate, 137 mM NaCl, 1 mM sodium vanadate, 1 mM phenylmethylsulfonyl fluoride, 10 µg/ml aprotinin, 1 µg/ml pepstatin, 5 µg/ml leupeptin and cleared of insoluble material by centrifugation at 10,000 x g for 10 min at 4°C for subsequent use. Human islets and MIN6 cells were stimulated with glucose as indicated and secreted insulin and insulin content was quantified using ELISA (Mercodia) and HTRF (Cisbio) assays. SK-MEL-2 cells stably expressing Smad or NFkB reporters were provided by the Whitehurst lab (49) and were grown in MEMα supplemented with 10% FBS and 100 units/ml penicillin, 100 µg/ml streptomycin.

Secreted Gaussia luciferase assays – Ins-GLuc-MIN6 cells were generated as previously described (14). Cells were plated in 96-well dishes at 1e5 cells/well and incubated for 2-3 days. Cells were then washed twice with KRBH and preincubated in 100 µl of KRBH (250 µM diazoxide included where indicated in figure legends) for 1 h. The buffer was then removed and cells were washed one time with 100 µl of KRBH and then incubated in KRBH with or without the indicated glucose concentration (or 200 □M

diazoxide, 35mM KCl, 20mM Glucose where indicated) for 1 h. 50 μl of KRBH was collected from each well and pipetted into a white opaque 96-well plate (Optiplate-96, Perkin-Elmer #6005290). Fresh GLuc assay working solution was then prepared by adding coelenterizine stock solution into assay buffer to a final concentration of 10 μM and the tube was wrapped in foil to protect from light. 50 μl of working solution was then rapidly added to the wells using a Matrix 125 μl electric multi-channel pipette for a final concentration of 5 μM. After adding reagent to the plate, luminescence was measured immediately on a Synergy2 H1 (BioTek) plate reader. The protocol was set to shake the plate orbitally for 3 seconds and then read the luminescence of each well with a 100 ms integration time.

Isolation of natural product fractions and bacterial strain information - The library of microbial and invertebrate natural product fractions was subjected to liquid chromatography-mass spectrometry (LC-MS) analysis using an Agilent Model 6130 single quadrupole mass spectrometer with a HP1200 HPLC. A photodiode array detector provided a chemical fingerprint of all fractions on the basis of molecular weight and UV profile. Fractions were dereplicated using various compound databases, including Antibase, Reaxys, and Scifinder Scholar. The sediment was desiccated and stamped onto agar plates using gauze 1 acidic media (20 g starch, 1 g $NaNO_3$, 0.5 g K_2HPO_4, 0.5 g $MgSO_4$, 0.5 g NaCl, 0.01 g $FeSO_4$, 10 μM cadaverine, 10 μM spermidine, 750 mL seawater, 15 g agar, pH adjusted to 5.3 with phosphate buffer). Bacterial colonies were selected and streaked for purity using the same agar media. Standard procedures for 16S rRNA analysis were used for phylogenetic

characterization of bacterial strains. Analysis of the Streptomyces sp. strain SN-B-022-1 by 16S rRNA revealed 99% identity to Streptomyces anulatus.

Cultivation and Extraction of SN-B-022-1 - Bacterium SN-B-022 was cultured in 5 × 2.8 L Fernbach flasks each containing 1 L of a seawater-based medium (10 g starch, 4 g yeast extract, 2 g peptone, 1 g $CaCO_3$, 40 mg $Fe_2(SO_4)_3 \cdot 4H_2O$, 100 mg KBr) and shaken at 200 rpm at 27°C. After 7 days of cultivation, sterilized XAD-7-HP resin (20 g/L) was added to adsorb organic chemicals produced by the bacterium, and the culture and resin were shaken at 200 rpm for 2 h. The resin was extracted with acetone and filtered through cheesecloth. The acetone-soluble portion was dried *in vacuo* to yield 2.0 g of extract.

Purification of chromomycin A2 from SN-B-022-1 - The extract (300 mg out of 2.0 g) was subjected to reversed-phase medium-pressure liquid chromatography (MPLC) with 5% CH_3OH/H_2O for 1 min, followed by a linear gradient of CH_3OH/H_2O from 5% to 100% over 15 min, 4 min of column washing with pure CH_3OH, and substitution of the column with 5% CH_3OH/H_2O for 2 min to provide 20 library fractions (SNB-022-1 to -20). Chromomycin A2 (1.2 mg, tR = 32.1 min) was obtained from the active fraction SN-B-022-1 (88 mg) by reversed-phase HPLC (5-µm, 10.0 mm × 250 mm) using 25% CH_3OH/H_2O (0.1% formic acid) for 5 min, followed by a linear gradient of CH_3OH/H_2O from 25% to 85% over 30 min, and 5 min of column washing with pure CH3CN. Application of the same HPLC purification method to SN-B-022-3 (14 mg) enabled isolation of additional samples of chromomycin A2 (2.6 mg). The compound was identified by comparison of NMR data to literature values (20), and the structure of

chromomycin A2 was confirmed independently through analysis of two-dimensional NMR (HSQC and HMBC) data.

Immunoblotting and Microscopy – 40-50 μg of cleared cell lysates were separated on 10% gels by SDS-PAGE and transferred to nitrocellulose for immunoblotting. All membranes were blocked in Odyssey blocking buffer (Licor) for 1 h before overnight incubation with primary antibodies diluted in blocking buffer. After three 10 min washes in 20 mM Tris-HCl pH 7.6, 150 mM NaCl, 0.1% Tween-20 (TBS-T), membranes were incubated with fluorescent secondary antibodies for 1 h at room temperature. After three 10 min washes in TBS-T, membranes were imaged on a Licor Odyssey scanner. For experiments where cells were fixed and stained with DAPI, MIN6 cells were plated in 96 well plates at 5e4 cells/well 24 h prior to treatment. After treatment, cells were fixed and permeabilized in 4% paraformaldehyde and 0.18% Triton-X100 in PBS pH 7.4 for 10 min, washed three times for 5 min each, and then stained with DAPI (300 nM) in PBS for 10 min. Plates were imaged using a GE®INCell 6000 automated microscope, 10X objective lens, and DAPI filters. Image analysis was performed using CellProfiler.

Quantitative PCR (RT-qPCR) – RNA was isolated from MIN6 cells using the PureLink RNA Mini Kit (Life Technologies). 1-2 μg of MIN6 RNA was converted into cDNA using the iScript kit (Bio-Rad) and the resulting cDNA was diluted 10-fold with water. Two μl of diluted cDNA were used in 20 μl qPCR reactions using 2X SYBR Bio-Rad master mix and 250 nM of each primer. qPCR data was analyzed using the Bio-Rad CFX Manager software. Primers used are listed in the **Table S1**.

Statistical Analysis – Quantitated data are expressed as mean ± SE. Data were evaluated using Student's t test, or two-way ANOVA where indicated, and considered significant if $P < 0.05$. Graphs were made in GraphPad Prism 6.

Acknowledgements

We would like to thank current and former members of the Cobb lab for helpful discussions. Mithramycin was a generous gift from Ralf Kittler. Early phases of this work were supported by a National Institutes of Health NRSA DK100113 (M.A.K.) and R01 DK55310 (M.H.C.). Other support was provided through U41 AT008718 (J.B.M.). We are grateful to the Welch Foundation for funding portions of this project (I1689 J.B.M., I1243 M.H.C.).

Figure Legends

Figure 1. Activity-guided fractionation identifies chromomycin A2 as an insulin secretion inhibitor.

A) Natural product subfractions from SNB-022-1 were tested for inhibitory activity in Ins-GLuc MIN6 β cells stimulated with the diazoxide (Dz) paradigm. Cells were treated overnight with fractions (10 μg/ml) or DMSO (0.1%); thapsigargin (Tg, 1 μM) was a positive control. Cells were preincubated in KRBH for 1 h followed by 1 h in the presence of either Dz (250 μM) or Dz + 40 mM KCl and 20 mM glucose. Secreted luciferase activity is shown.

B) Ins-GLuc MIN6 cells were treated overnight with different doses of CMA2 followed by a glucose-stimulated secretion assay and the resulting RLUs were used to determine the EC_{50}. Data are the mean ± SE of four independent experiments.

C) Ins-GLuc MIN6 cells were treated with CMA2 (100 nM) starting at the beginning of the 1 h KRBH preincubation and during the 1 h glucose (20 mM) stimulation. Secreted luciferase activity was measured at the end of the assay. Data represent the mean ± SE of three independent experiments performed in triplicate.

D) Human islets were hand-picked into groups of 50 and treated overnight with CMA2 at the indicated doses in 500 μl of complete CMRL media. The islets were then subjected to static glucose-stimulated insulin secretion assays and the secreted and total insulin concentrations were measured. Data are the mean ± SD of two batches of donor islets.

E, F) MIN6 cells were treated overnight with CMA2 (100 nM) and then prepared for calcium influx measurements using Fura-PE3 (5 μM). In (**E**) cells were preincubated in KRBH without glucose for 1 h, loaded with Fura-PE3 for 30 min, followed by a baseline calcium measurement for 5 min. 20 mM glucose was added and Fura fluorescence was measured for 30 min. In (**F**), diazoxide (250 μM) was included in the KRBH during the baseline reading and throughout the stimulation protocol. Data are shown as traces representing the mean ± SE (shown as dots) from three independent passages of MIN6 cells.

G) MIN6 cells were treated overnight with DMSO (0.1%) or CMA2 (100 nM) and the next day incubated 2 h in KRBH without glucose, but containing either DMSO or CMA2. Cells were then stimulated with 20 mM glucose for 5 and 30 min and cells were lysed for immunoblotting against pERK1/2, ERK1/2 and pS235/6-S6, and S6. Bar graphs of quantified immunoblots are show and data are the mean ± SE of at least three independent experiments. Using two-way ANOVA: *a*, $P<0.05$ vs respective glucose 0 min. *b*, $P<0.05$ vs control, n.s., not signficant vs respective glucose 0 min.

Figure 2. Overnight treatment with CMA2 causes dysregulated basal ATP concentrations but does not prevent glucose-stimulated calcium influx.

A) After an overnight treatment with CMA2 or MTM at the indicated doses, Ins-GLuc MIN6 cells were preincubated in KRBH without glucose for 1 h and then incubated with diazoxide (Dz) (250 μM) for 1 h for the experiment in 1C. After the experiment, the cells were lysed in passive lysis buffer containing Cell Titer Glo reagent to measure the relative abundance of ATP. Data are the mean ± SE of three independent experiments.

B) MIN6 cells were treated overnight with DMSO (0.1%) or CMA2 (100 nM)

Figure 3. CMA2 has distinct effects on β cells compared to the analog mithramycin.

A) Ins-GLuc MIN6 cells were treated overnight with either CMA2 or mithramycin (MTM) at the indicated doses and then secretion was stimulated using the diazoxide (Dz) paradigm as previously. Secreted luciferase activity was measured and the data are the mean ± SE from three independent experiments. *, P<0.05 by two-way ANOVA.

B) Lysates of the diazoxide-treated samples in (**A**) were subjected to Cell Titer Glo assays to measure viability. The luciferase activity is shown with respect to DMSO control and the data are the mean ± SE of three independent experiments.

C) MIN6 cells were treated with CMA2 overnight and RNA was isolated for RT-qPCR against INSI/II, PDX1, and UCN3. Data were normalized to 18S rRNA by the $2^{-\Delta\Delta Ct}$ method and are the mean ± SE of three independent experiments. *,P<0.05 vs DMSO control.

Figure S1.

A) Nuclear magnetic resonance spectra of the purified compound from fraction SNB-022-1. B) The spectra in (A) matched chromomycin A2 and the structure is shown. The structure of the closely related mithramycin is shown as well for comparison.

Figure S2.

SK-MEL2 cell lines stably expressing luciferase reporters for Smad (**A**) or NFkB (**B**) were stimulated with TGFβ or TNFα, respectively, at the indicated doses for 24 h. The cells were then lysed in passive lysis buffer and analyzed in a Firefly luciferase assay. The data represent the mean ± SD of two independent experiments performed in duplicate. **C**) Insulin content was measured in lysates from MIN6 cells that were treated overnight with CMA2 (100 nM) or DMSO (0.1%). Data are the mean ± SE of three independent experiments. **D**) MIN6 cells were treated with the indicated doses of CMA2 for 72 h and subjected to a Cell Titer Glo assay to measure viability. Data are the mean ± SE normalized to the percent of DMSO for three independent experiments. *, $P<0.05$ vs DMSO. **E**) The data in (**D**) were confirmed by treating MIN6 cells with CMA2 for 48 h followed by fixation and staining with DAPI. Nuclei counts per well are shown as the mean ± SE for three independent passages of cells. *,$P<0.05$ vs DMSO.

References:

1. (2017) *Centers for Disease Control and Prevention. National Diabetes Statistics Report*,
2. Stanley, C. A. (2011) Two genetic forms of hyperinsulinemic hypoglycemia caused by dysregulation of glutamate dehydrogenase. *Neurochem Int* **59**, 465-472
3. Molven, A., Matre, G. E., Duran, M., Wanders, R. J., Rishaug, U., Njolstad, P. R., Jellum, E., and Sovik, O. (2003) Familial Hyperinsulinemic Hypoglycemia Caused by a Defect in the SCHAD Enzyme of Mitochondrial Fatty Acid Oxidation. *Diabetes* **53**, 221-227

4. Cordain, L., Eades, M. R., and Eades, M. D. (2003) Hyperinsulinemic diseases of civilization: more than just Syndrome X. *Comparative Biochemistry and Physiology Part A: Molecular & Integrative Physiology* **136**, 95-112
5. Hansen, J., G. Arkhammar, P., Bodvarsdottir, T., and Wahl, P. (2004) Inhibition of Insulin Secretion as a New Drug Target in the Treatment of Metabolic Disorders. *Current Medicinal Chemistry* **11**, 1595-1615
6. Henquin, J. C., Dufrane, D., Gmyr, V., Kerr-Conte, J., and Nenquin, M. (2017) Pharmacological approach to understanding the control of insulin secretion in human islets. *Diabetes, obesity & metabolism* **19**, 1061-1070
7. Henquin, J. C. (2009) Regulation of insulin secretion: a matter of phase control and amplitude modulation. *Diabetologia* **52**, 739-751
8. Hu, Y., Espindola, A. P., Stewart, N. A., Wei, S., Posner, B. A., and MacMillan, J. B. (2011) Chromomycin SA analogs from a marine-derived Streptomyces sp. *Bioorg Med Chem* **19**, 5183-5189
9. Vaden, R. M., Oswald, N. W., Potts, M. B., MacMillan, J. B., and White, M. A. (2017) FUSION-Guided Hypothesis Development Leads to the Identification of N(6),N(6)-Dimethyladenosine, a Marine-Derived AKT Pathway Inhibitor. *Mar Drugs* **15**
10. Potts, M. B., McMillan, E. A., Rosales, T. I., Kim, H. S., Ou, Y. H., Toombs, J. E., Brekken, R. A., Minden, M. D., MacMillan, J. B., and White, M. A. (2015) Mode of action and pharmacogenomic biomarkers for exceptional responders to didemnin B. *Nature chemical biology* **11**, 401-408
11. Potts, M. B., Kim, H. S., Fisher, K. W., Hu, Y., Carrasco, Y. P., Bulut, G. B., Ou, Y. H., Herrera-Herrera, M. L., Cubillos, F., Mendiratta, S., Xiao, G., Hofree, M., Ideker, T., Xie, Y., Huang, L. J., Lewis, R. E., MacMillan, J. B., and White, M. A. (2013) Using functional signature ontology (FUSION) to identify mechanisms of action for natural products. *Sci Signal* **6**, ra90
12. Elkin, S. R., Oswald, N. W., Reed, D. K., Mettlen, M., MacMillan, J. B., and Schmid, S. L. (2016) Ikarugamycin: A Natural Product Inhibitor of Clathrin-Mediated Endocytosis. *Traffic* **17**, 1139-1149
13. Hu, Y., Wang, K., and MacMillan, J. B. (2013) Hunanamycin A, an antibiotic from a marine-derived Bacillus hunanensis. *Org Lett* **15**, 390-393
14. Kalwat, M. A., Wichaidit, C., Nava Garcia, A. Y., McCoy, M. K., McGlynn, K., Hwang, I. H., MacMillan, J. B., Posner, B. A., and Cobb, M. H. (2016) Insulin promoter-driven Gaussia luciferase-based insulin secretion biosensor assay for discovery of beta-cell glucose-sensing pathways. *ACS Sens* **1**, 1208-1212
15. Lombo, F., Menendez, N., Salas, J. A., and Mendez, C. (2006) The aureolic acid family of antitumor compounds: structure, mode of action, biosynthesis, and novel derivatives. *Appl Microbiol Biotechnol* **73**, 1-14
16. Hou, C., Weidenbach, S., Cano, K. E., Wang, Z., Mitra, P., Ivanov, D. N., Rohr, J., and Tsodikov, O. V. (2016) Structures of mithramycin analogues bound to DNA and implications for targeting transcription factor FLI1. *Nucleic acids research* **44**, 8990-9004
17. Sobell, H. M. (1985) Actinomycin and DNA transcription. *Proceedings of the National Academy of Sciences* **82**, 5328-5331

18. Bushnell, D. A., Cramer, P., and Kornberg, R. D. (2002) Structural basis of transcription: alpha-amanitin-RNA polymerase II cocrystal at 2.8 A resolution. *Proceedings of the National Academy of Sciences of the United States of America* **99**, 1218-1222
19. Singh, D. K., Kollipara, R. K., Vemireddy, V., Yang, X. L., Sun, Y., Regmi, N., Klingler, S., Hatanpaa, K. J., Raisanen, J., Cho, S. K., Sirasanagandla, S., Nannepaga, S., Piccirillo, S., Mashimo, T., Wang, S., Humphries, C. G., Mickey, B., Maher, E. A., Zheng, H., Kim, R. S., Kittler, R., and Bachoo, R. M. (2017) Oncogenes Activate an Autonomous Transcriptional Regulatory Circuit That Drives Glioblastoma. *Cell Rep* **18**, 961-976
20. Toume, K., Tsukahara, K., Ito, H., Arai, M. A., and Ishibashi, M. (2014) Chromomycins A2 and A3 from marine actinomycetes with TRAIL resistance-overcoming and Wnt signal inhibitory activities. *Mar Drugs* **12**, 3466-3476
21. Simon, H., Wittig, B., and Zimmer, C. (1994) Effect of netropsin, distamycin A and chromomycin A3on the binding and cleavage reaction of DNA gyrase. *FEBS Letters* **353**, 79-83
22. Guimaraes, L. A., Jimenez, P. C., Sousa Tda, S., Freitas, H. P., Rocha, D. D., Wilke, D. V., Martin, J., Reyes, F., Deusdenia Loiola Pessoa, O., and Costa-Lotufo, L. V. (2014) Chromomycin A2 induces autophagy in melanoma cells. *Mar Drugs* **12**, 5839-5855
23. Ratovitski, E. A. (2016) Tumor Protein (TP)-p53 Members as Regulators of Autophagy in Tumor Cells upon Marine Drug Exposure. *Mar Drugs* **14**
24. McMillan, E. A., Kwon, S., Clemenceau, J. R., Fisher, K. W., Vaden, R. M., Neilsen, B. K., Shaikh, A., Kelly, D., Potts., M. B., Mendiratta, S., Sung, Y., MacMillan, J. B., Lewis, R. E., Kim, H. K., and White, M. A. (2018) A genome wide functional signature ontology map (FuSiOn) and applications to natural product mechanism of action discovery. *In submission at Cell Systems*
25. Das, B., Neilsen, B. K., Fisher, K. W., Gehring, D., Hu, Y., Volle, D. J., Kim, H. S., McCall, J. L., Kelly, D. L., MacMillan, J. B., White, M. A., and Lewis, R. E. (2018) A Functional Signature Ontology (FUSION) screen detects an AMPK inhibitor with selective toxicity toward human colon tumor cells. *Sci Rep* **8**, 3770
26. Liu, Z., and Habener, J. F. (2010) Wnt signaling in pancreatic islets. *Adv Exp Med Biol* **654**, 391-419
27. Sorrenson, B., Cognard, E., Lee, K. L., Dissanayake, W. C., Fu, Y., Han, W., Hughes, W. E., and Shepherd, P. R. (2016) A Critical Role for beta-catenin in Modulating Levels of Insulin Secretion from beta-cells by Regulating Actin Cytoskeleton and Insulin Vesicle Localization. *The Journal of biological chemistry*
28. Welters, H. J., and Kulkarni, R. N. (2008) Wnt signaling: relevance to beta-cell biology and diabetes. *Trends Endocrinol Metab* **19**, 349-355
29. Bader, E., Migliorini, A., Gegg, M., Moruzzi, N., Gerdes, J., Roscioni, S. S., Bakhti, M., Brandl, E., Irmler, M., Beckers, J., Aichler, M., Feuchtinger, A., Leitzinger, C., Zischka, H., Wang-Sattler, R., Jastroch, M., Tschop, M., Machicao, F., Staiger, H., Haring, H. U., Chmelova, H., Chouinard, J. A., Oskolkov, N., Korsgren, O., Speier, S., and Lickert, H. (2016) Identification of proliferative and mature beta-cells in the islets of Langerhans. *Nature* **535**, 430-434

30. Kalwat, M. A., and Cobb, M. H. (2017) Mechanisms of the amplifying pathway of insulin secretion in the beta cell. *Pharmacol Ther* **179**, 17-30
31. Henquin, J. C. (2000) Triggering and amplifying pathways of regulation of insulin secretion by glucose. *Diabetes* **49**, 1751-1760
32. Leduc, M., Richard, J., Costes, S., Muller, D., Varrault, A., Compan, V., Mathieu, J., Tanti, J. F., Pages, G., Pouyssegur, J., Bertrand, G., Dalle, S., and Ravier, M. A. (2017) ERK1 is dispensable for mouse pancreatic beta cell function but is necessary for glucose-induced full activation of MSK1 and CREB. *Diabetologia* **60**, 1999-2010
33. Wauson, E. M., Guerra, M. L., Dyachok, J., McGlynn, K., Giles, J., Ross, E. M., and Cobb, M. H. (2015) Differential Regulation of ERK1/2 and mTORC1 Through T1R1/T1R3 in MIN6 Cells. *Mol Endocrinol* **29**, 1114-1122
34. Lawrence, M. C., McGlynn, K., Park, B. H., and Cobb, M. H. (2005) ERK1/2-dependent activation of transcription factors required for acute and chronic effects of glucose on the insulin gene promoter. *The Journal of biological chemistry* **280**, 26751-26759
35. Khoo, S., Griffen, S. C., Xia, Y., Baer, R. J., German, M. S., and Cobb, M. H. (2003) Regulation of insulin gene transcription by ERK1 and ERK2 in pancreatic beta cells. *The Journal of biological chemistry* **278**, 32969-32977
36. Guerra, M. L., Kalwat, M. A., McGlynn, K., and Cobb, M. H. (2017) Sucralose activates an ERK1/2-ribosomal protein S6 signaling axis. *FEBS Open Bio* **7**, 174-186
37. Moore, C. E., Xie, J., Gomez, E., and Herbert, T. P. (2009) Identification of cAMP-dependent kinase as a third in vivo ribosomal protein S6 kinase in pancreatic beta-cells. *Journal of molecular biology* **389**, 480-494
38. Kuleshov, M. V., Jones, M. R., Rouillard, A. D., Fernandez, N. F., Duan, Q., Wang, Z., Koplev, S., Jenkins, S. L., Jagodnik, K. M., Lachmann, A., McDermott, M. G., Monteiro, C. D., Gundersen, G. W., and Ma'ayan, A. (2016) Enrichr: a comprehensive gene set enrichment analysis web server 2016 update. *Nucleic acids research* **44**, W90-97
39. van der Meulen, T., Donaldson, C. J., Caceres, E., Hunter, A. E., Cowing-Zitron, C., Pound, L. D., Adams, M. W., Zembrzycki, A., Grove, K. L., and Huising, M. O. (2015) Urocortin3 mediates somatostatin-dependent negative feedback control of insulin secretion. *Nat Med* **21**, 769-776
40. van der Meulen, T., Xie, R., Kelly, O. G., Vale, W. W., Sander, M., and Huising, M. O. (2012) Urocortin 3 marks mature human primary and embryonic stem cell-derived pancreatic alpha and beta cells. *PLoS One* **7**, e52181
41. Osgood, C. L., Maloney, N., Kidd, C. G., Kitchen-Goosen, S., Segars, L., Gebregiorgis, M., Woldemichael, G. M., He, M., Sankar, S., Lessnick, S. L., Kang, M., Smith, M., Turner, L., Madaj, Z. B., Winn, M. E., Nunez, L. E., Gonzalez-Sabin, J., Helman, L. J., Moris, F., and Grohar, P. J. (2016) Identification of Mithramycin Analogues with Improved Targeting of the EWS-FLI1 Transcription Factor. *Clinical cancer research : an official journal of the American Association for Cancer Research* **22**, 4105-4118

42. Gupta, R. S. (1982) Species specific differences in the toxicity of mithramycin, chromomycin A3, and olivomycin towards cultured mammalian cells. *Journal of cellular physiology* **113**, 11-16
43. Snider, K. E., Becker, S., Boyajian, L., Shyng, S. L., MacMullen, C., Hughes, N., Ganapathy, K., Bhatti, T., Stanley, C. A., and Ganguly, A. (2013) Genotype and phenotype correlations in 417 children with congenital hyperinsulinism. *J Clin Endocrinol Metab* **98**, E355-363
44. van Boekel, G., Loves, S., van Sorge, A., Ruinemans-Koerts, J., Rijnders, T., and de Boer, H. (2008) Weight loss in obese men by caloric restriction and high-dose diazoxide-mediated insulin suppression. *Diabetes, obesity & metabolism* **10**, 1195-1203
45. Brown, R. J., and Rother, K. I. (2008) Effects of beta-cell rest on beta-cell function: a review of clinical and preclinical data. *Pediatr Diabetes* **9**, 14-22
46. Nijhoff, M., Carlotti, F., Engelse, M., and de, K. E. (2018) Diazoxide pretreatment improves pancreatic islet survival in vitro and functionality in vivo. *Endocrine Abstracts*
47. Finke, E. H., Lacy, P. E., and Ono, J. (1979) Use of reflected green light for specific identification of islets in vitro after collagenase isolation. *Diabetes* **28**, 612-613
48. Kalwat, M. A., Huang, Z., Wichaidit, C., McGlynn, K., Earnest, S., Savoia, C., Dioum, E. M., Schneider, J. W., Hutchison, M. R., and Cobb, M. H. (2016) Isoxazole Alters Metabolites and Gene Expression, Decreasing Proliferation and Promoting a Neuroendocrine Phenotype in beta-Cells. *ACS chemical biology* **11**, 1128-1136
49. Maxfield, K. E., Taus, P. J., Corcoran, K., Wooten, J., Macion, J., Zhou, Y., Borromeo, M., Kollipara, R. K., Yan, J., Xie, Y., Xie, X. J., and Whitehurst, A. W. (2015) Comprehensive functional characterization of cancer-testis antigens defines obligate participation in multiple hallmarks of cancer. *Nat Commun* **6**, 8840

Figure 1

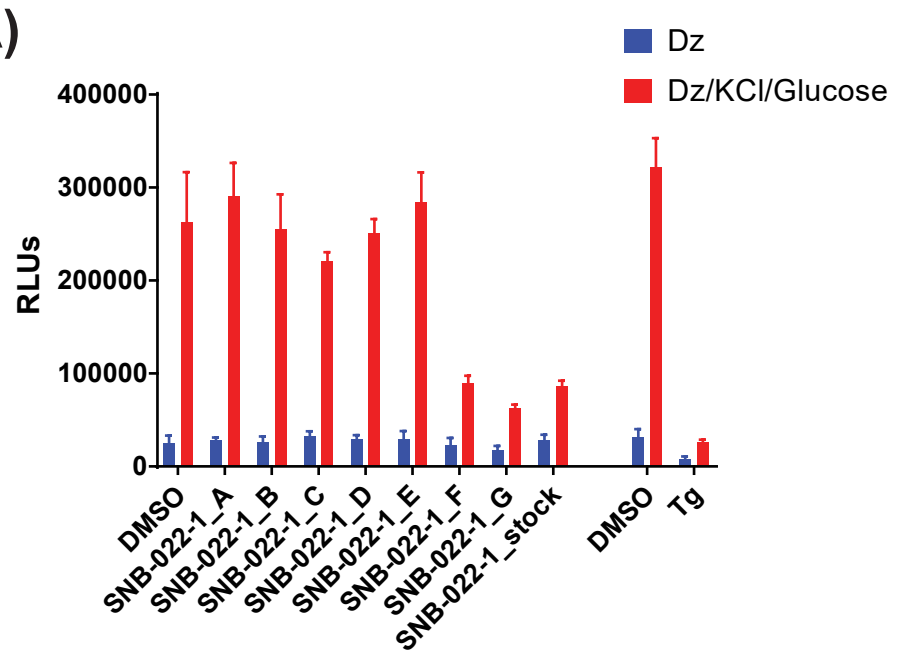

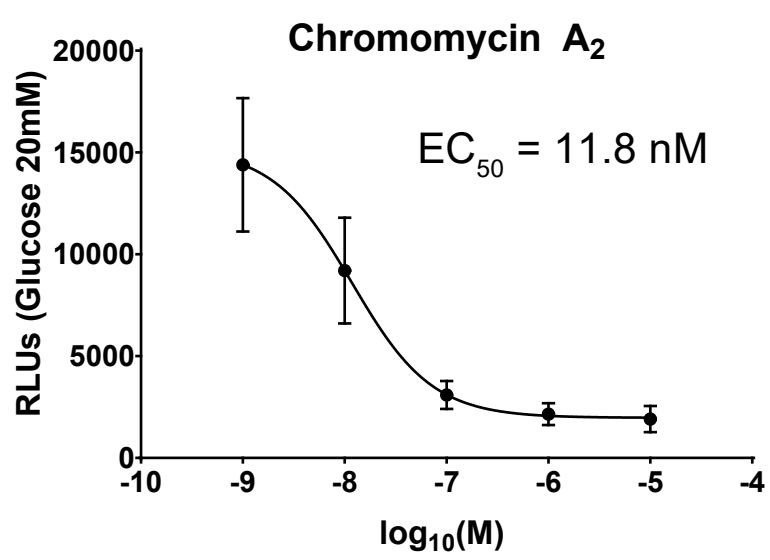

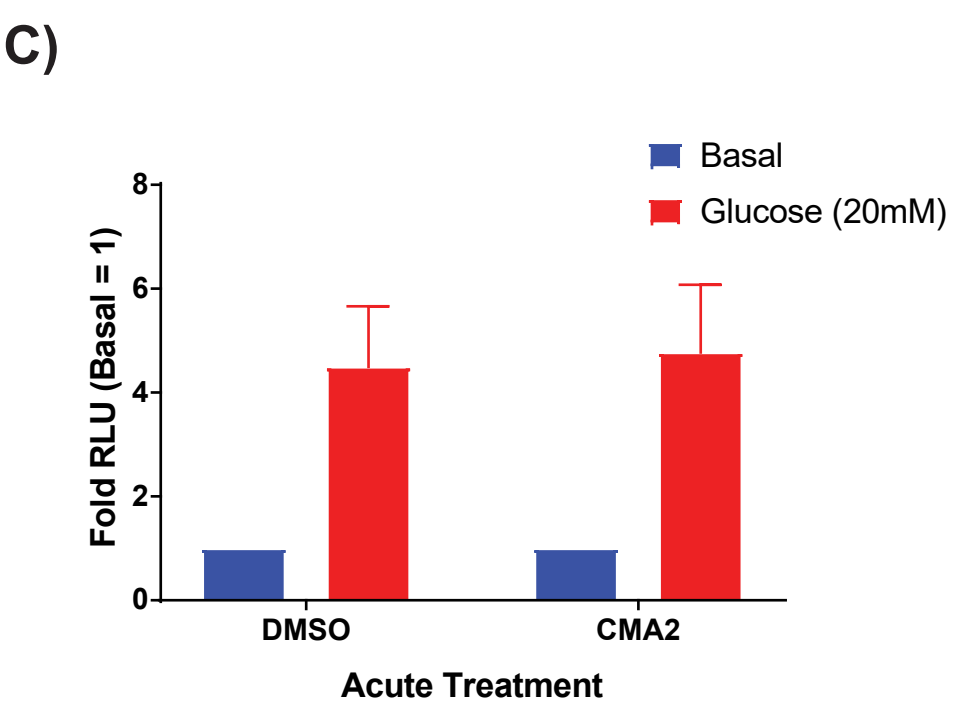

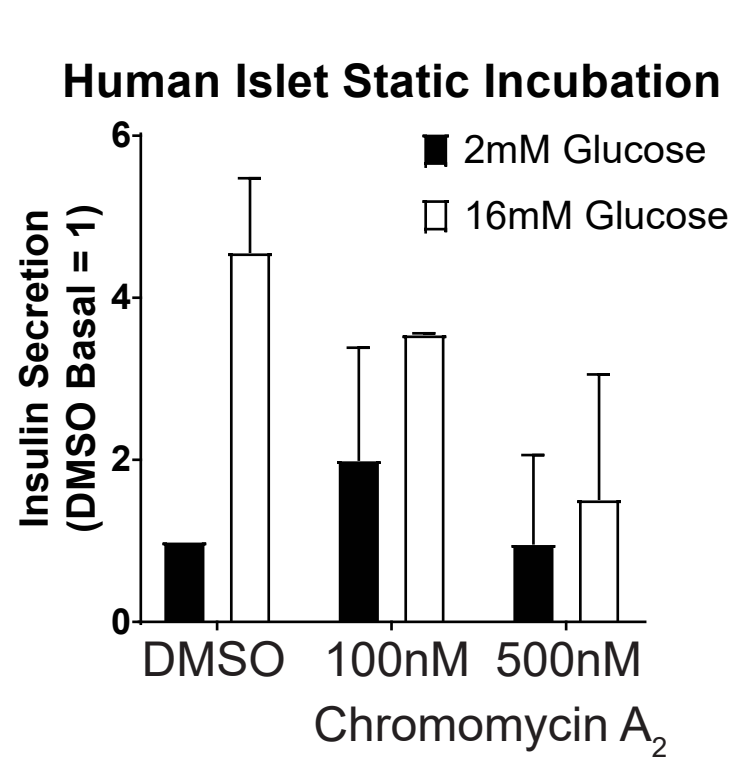

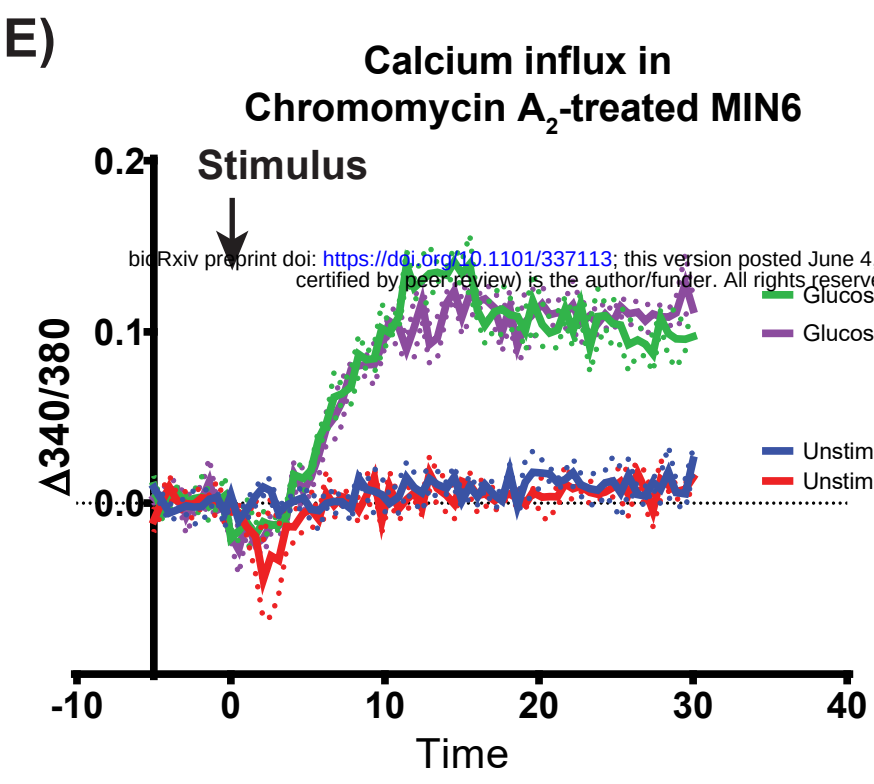

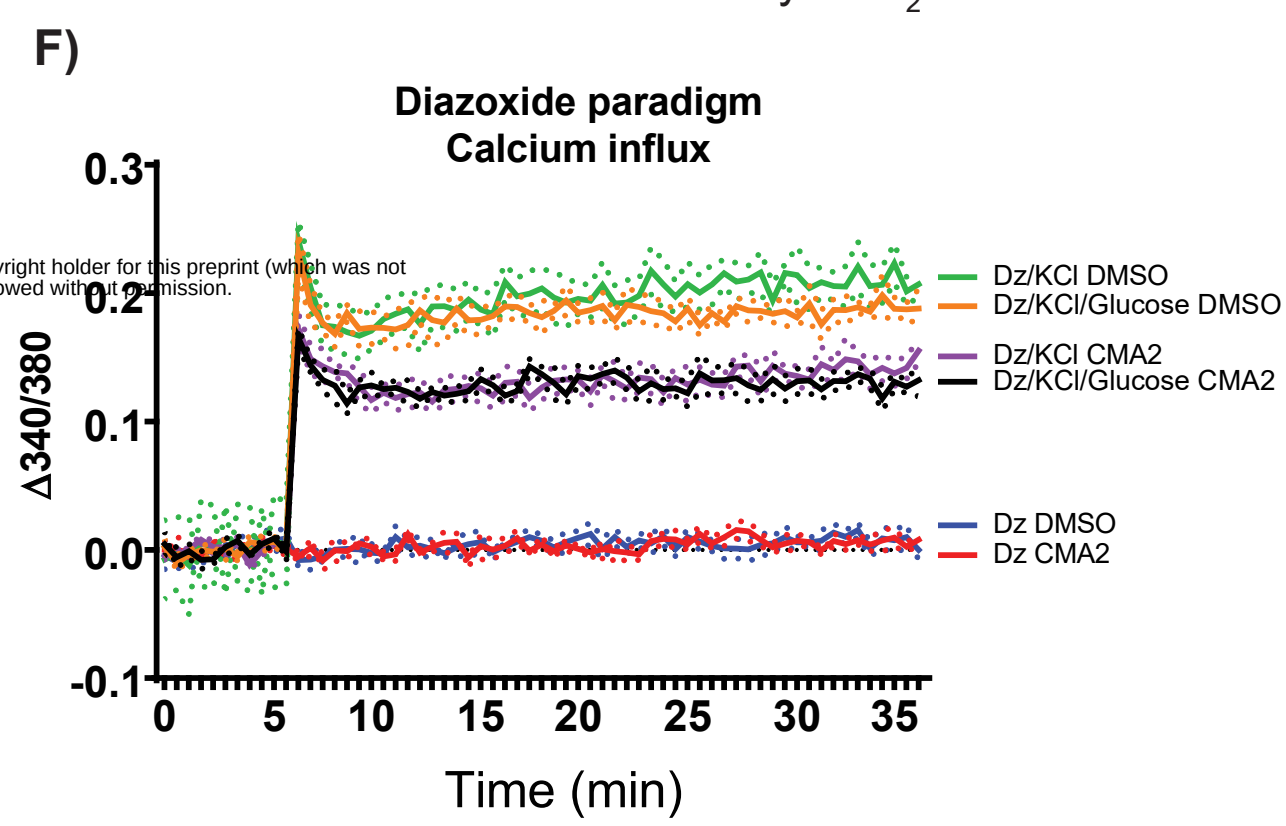

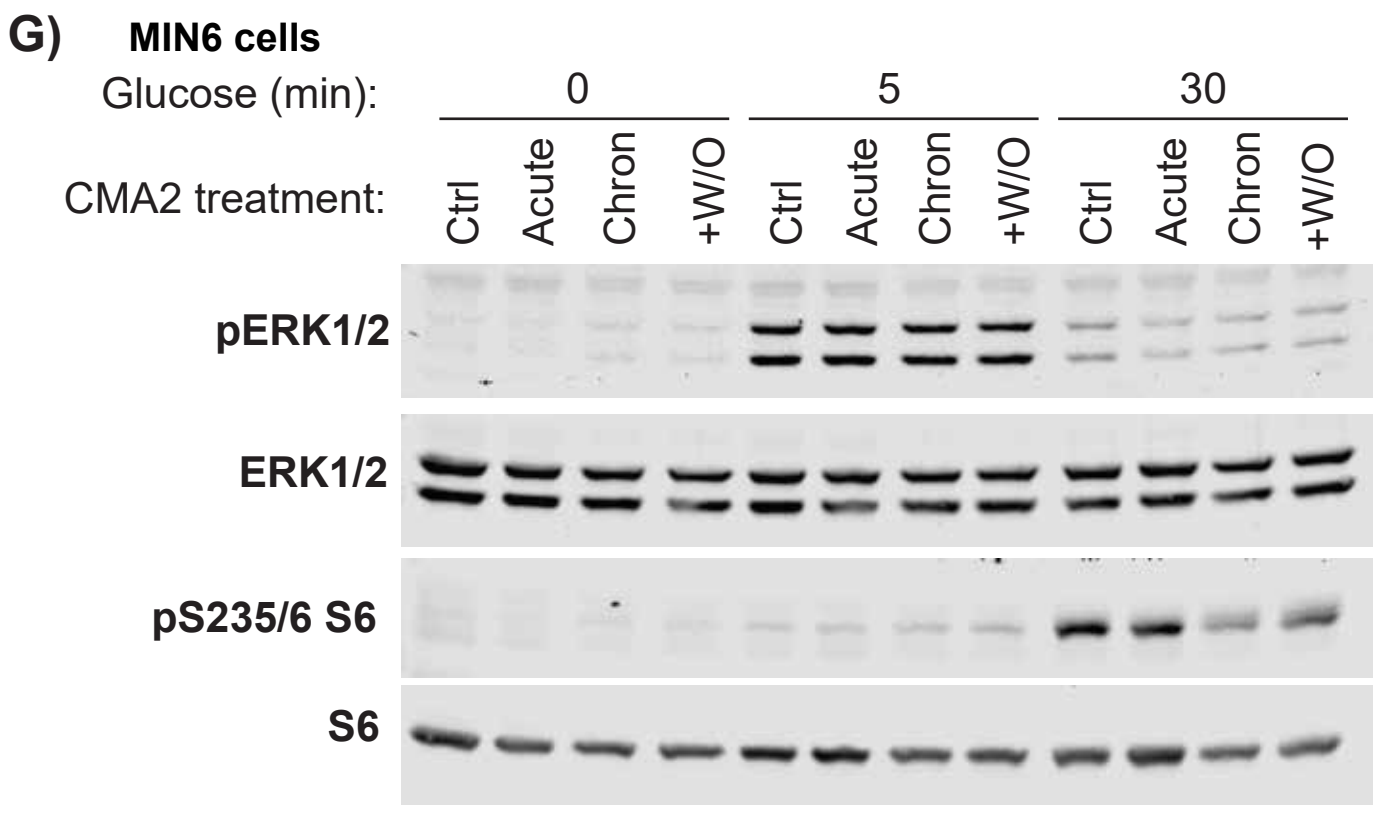

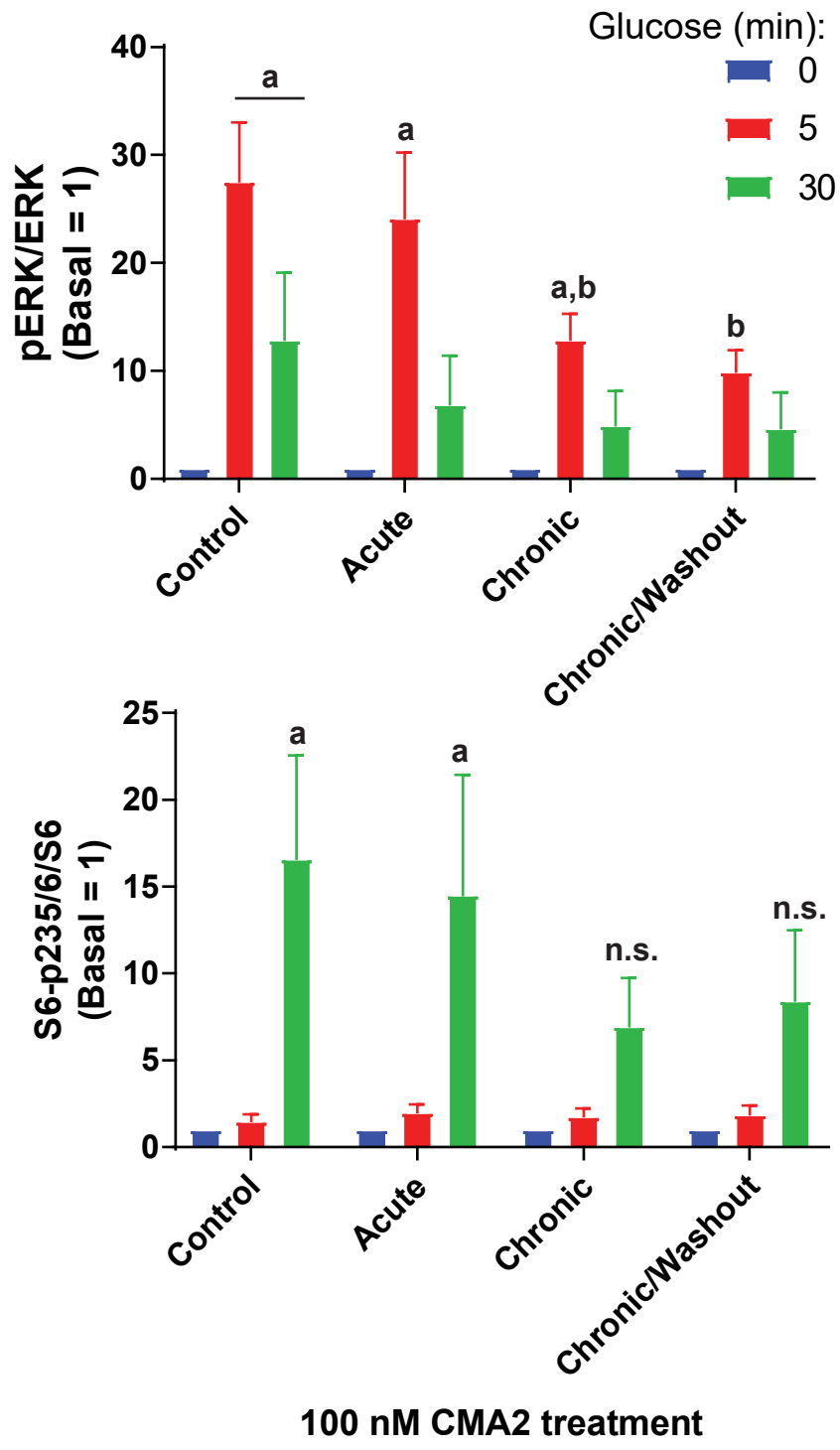

Figure 2

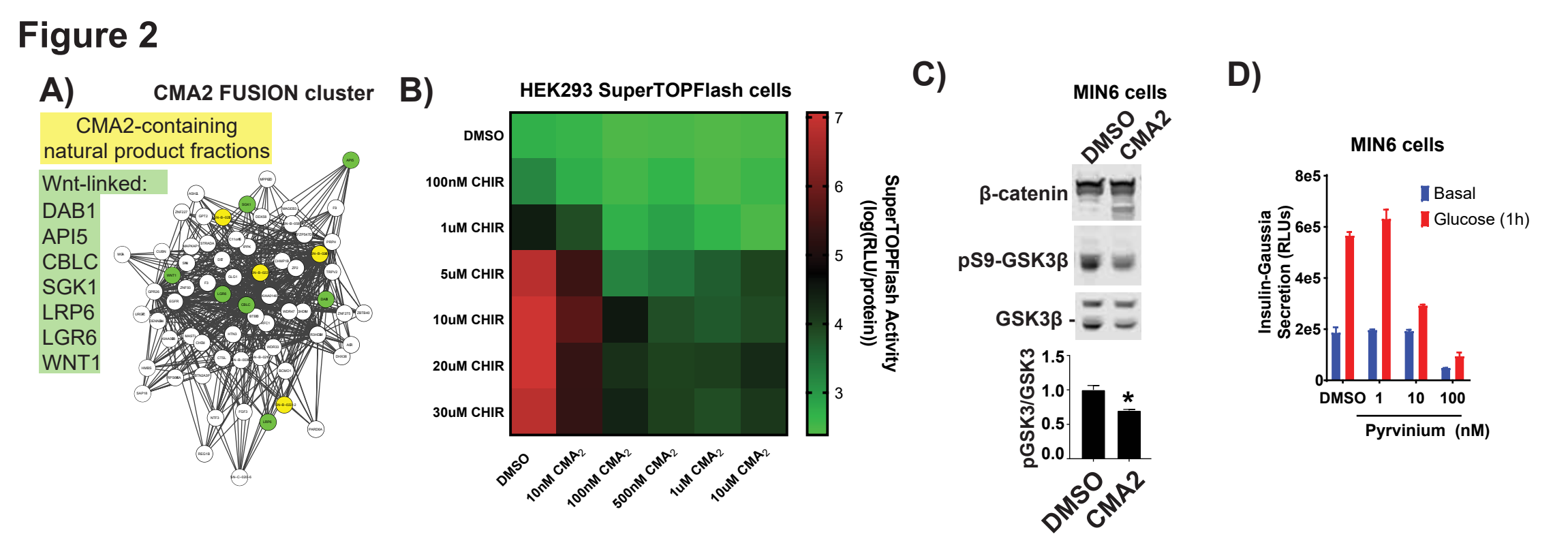
A)
CMA2 FUSION cluster
CMA2-containing natural product fractions
Wnt-linked:
DAB1
API5
CBLC
SGK1
LRP6
LGR6
WNT1
B)
HEK293 SuperTOPFlash cells
DMSO
100nM CHIR
1uM CHIR
5uM CHIR
10uM CHIR
20uM CHIR
30uM CHIR
DMSO
10nM CMA2
100nM CMA2
500nM CMA2
1uM CMA2
10uM CMA2
7
6
5
4
3
SuperTOPFlash Activity (log(RLU/protein))
C)
MIN6 cells
DMSO
CMA2
β-catenin
pS9-GSK3β
GSK3β -
pGSK3/GSK3
1.5
1.0
0.5
0.0
*
DMSO
CMA2
D)
MIN6 cells
Basal
Glucose (1h)
Insulin-Gaussia Secretion (RLUs)
8e5
6e5
4e5
2e5
0
DMSO
1
10
100
Pyrvinium (nM)

Figure 3

A)

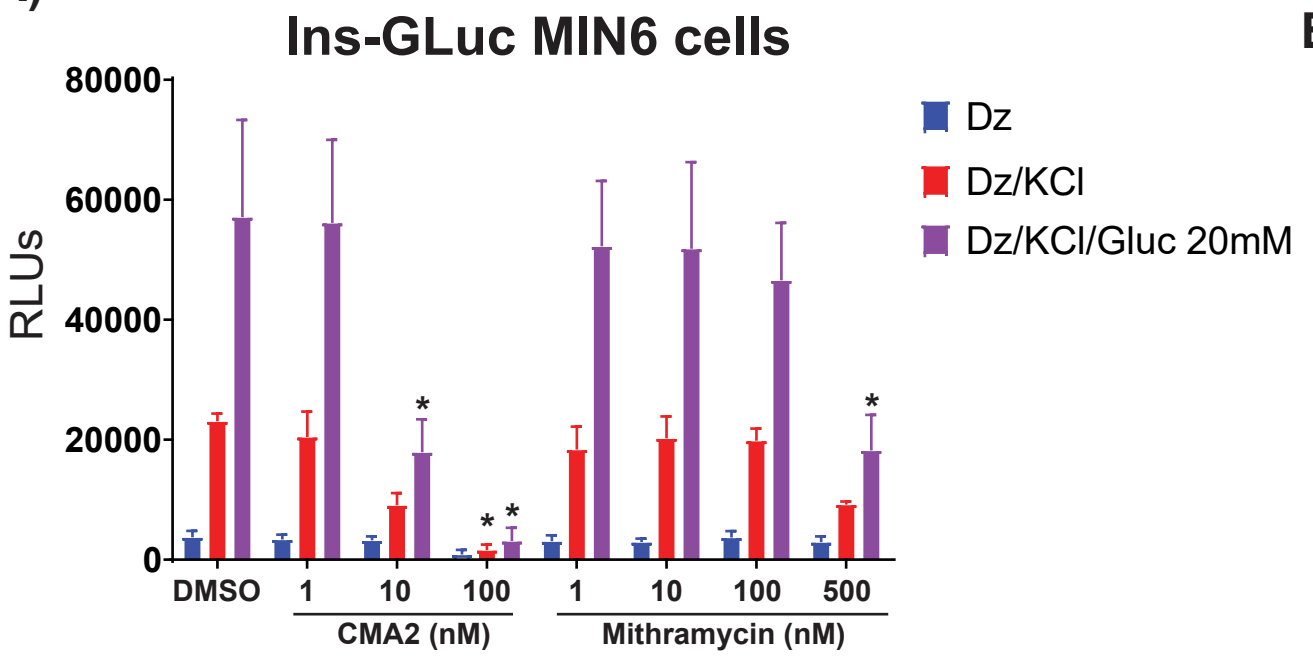
Ins-GLuc MIN6 cells
RLUs
80000
60000
40000
20000
0
Dz
Dz/KCl
Dz/KCl/Gluc 20mM
DMSO
1
10
100
1
10
100
500
CMA2 (nM)
Mithramycin (nM)
*

B)

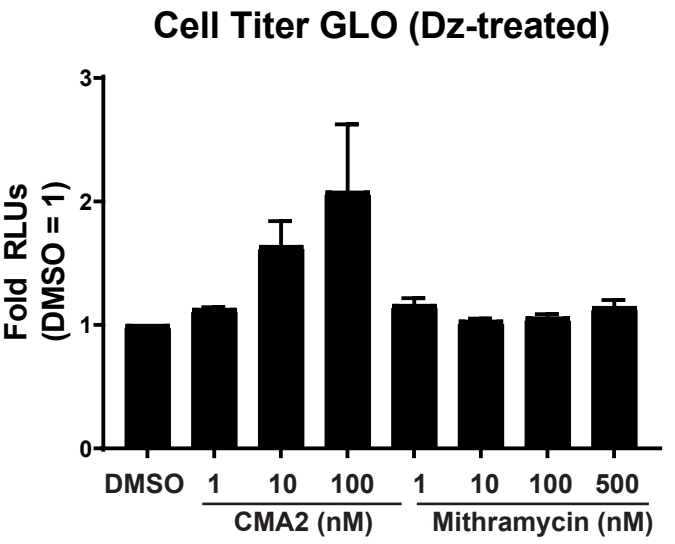
Cell Titer GLO (Dz-treated)
Fold RLUs (DMSO = 1)
3
2
1
0
DMSO
1
10
100
1
10
100
500
CMA2 (nM)
Mithramycin (nM)

C)

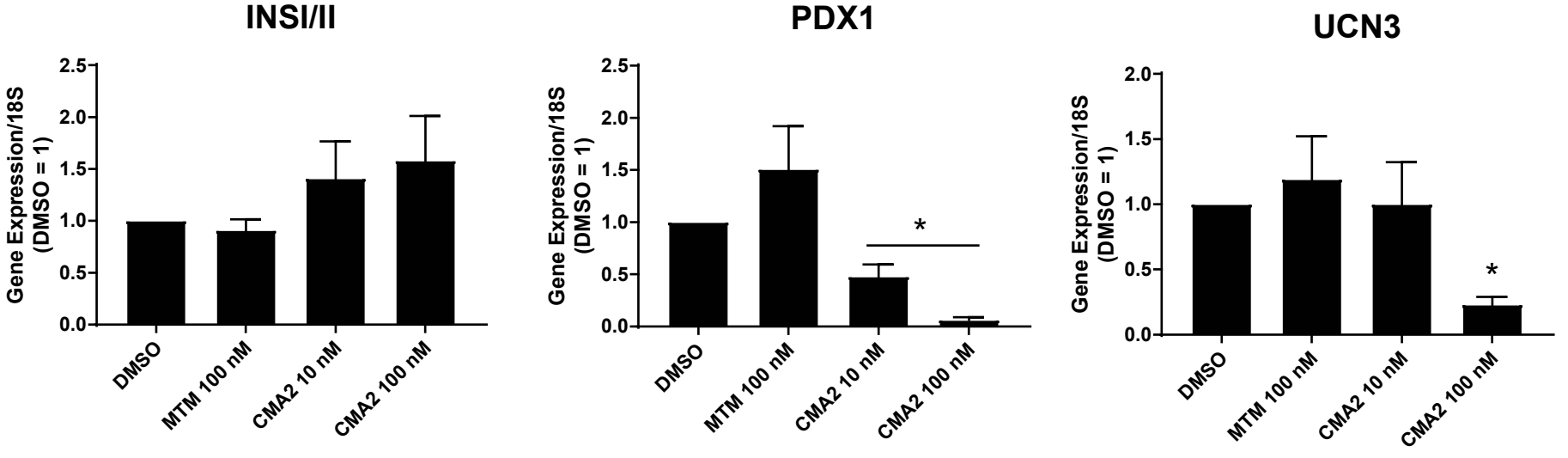
INSI/II
PDX1
UCN3
Gene Expression/18S (DMSO = 1)
DMSO
MTM 100 nM
CMA2 10 nM
CMA2 100 nM
*

Figure S1

A)

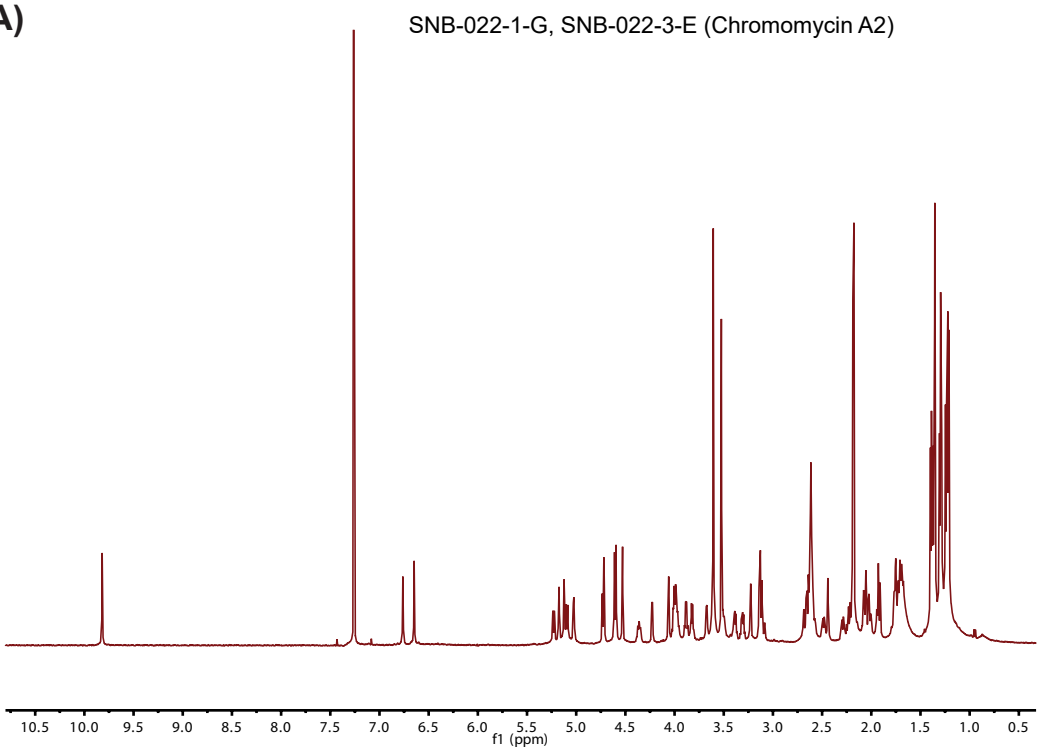
SNB-022-1-G, SNB-022-3-E (Chromomycin A2)
10.5 10.0 9.5 9.0 8.5 8.0 7.5 7.0 6.5 6.0 5.5 5.0 4.5 4.0 3.5 3.0 2.5 2.0 1.5 1.0 0.5
f1 (ppm)

B)

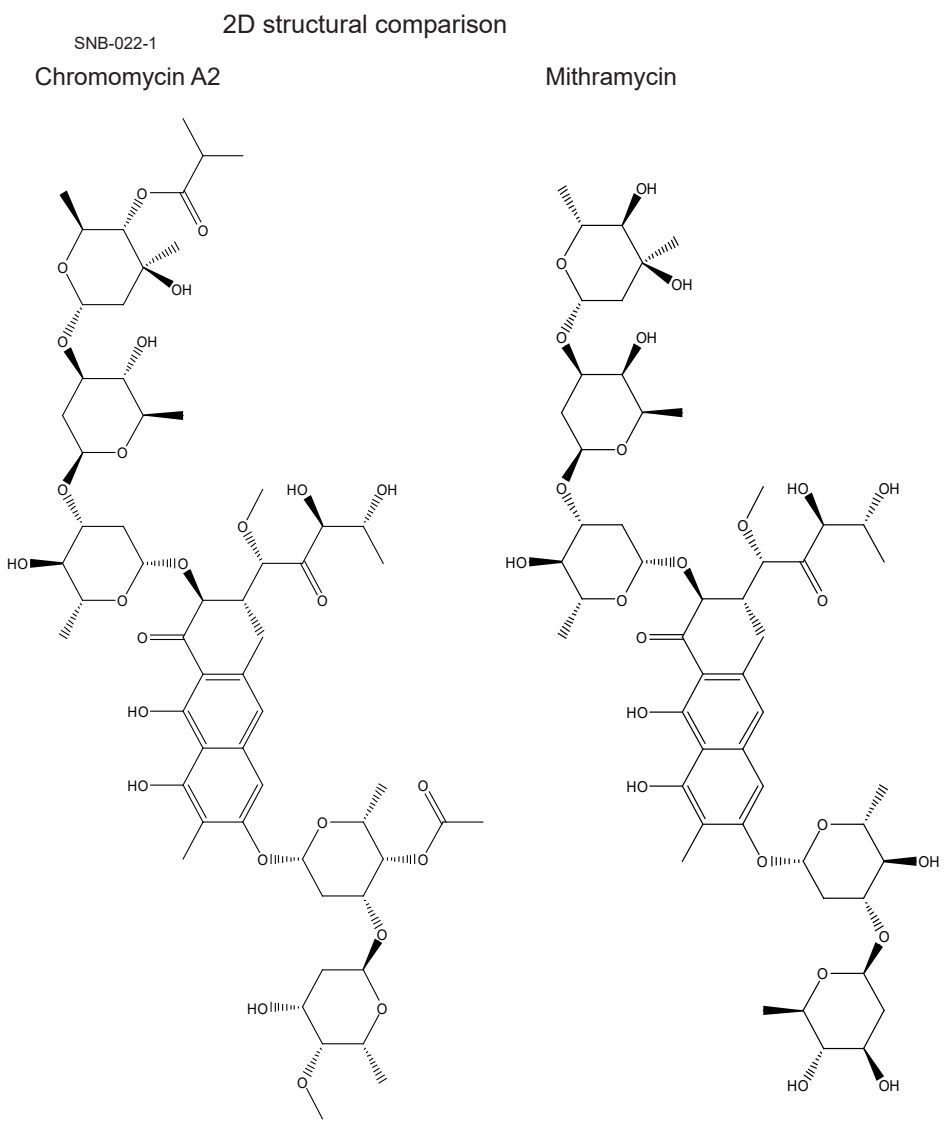
2D structural comparison
SNB-022-1
Chromomycin A2
Mithramycin

Figure S2

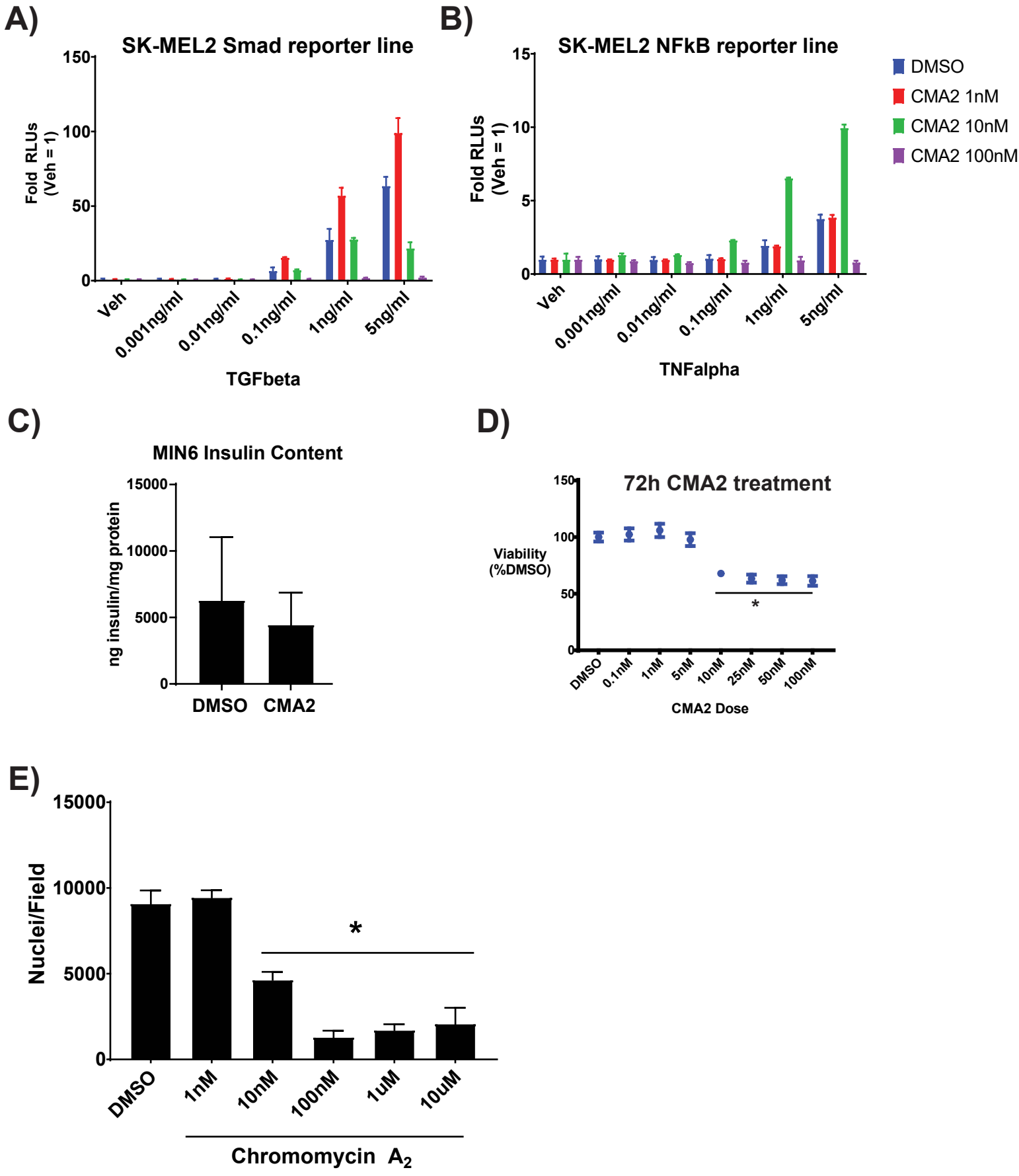
A)
SK-MEL2 Smad reporter line
Fold RLUs (Veh = 1)
150
100
50
0
Veh
0.001ng/ml
0.01ng/ml
0.1ng/ml
1ng/ml
5ng/ml
TGFbeta
B)
SK-MEL2 NFkB reporter line
Fold RLUs (Veh = 1)
15
10
5
0
Veh
0.001ng/ml
0.01ng/ml
0.1ng/ml
1ng/ml
5ng/ml
TNFalpha
DMSO
CMA2 1nM
CMA2 10nM
CMA2 100nM
C)
MIN6 Insulin Content
ng insulin/mg protein
15000
10000
5000
0
DMSO
CMA2
D)
72h CMA2 treatment
Viability (%DMSO)
150
100
50
0
*
DMSO
0.1nM
1nM
5nM
10nM
25nM
50nM
100nM
CMA2 Dose
E)
Nuclei/Field
15000
10000
5000
0
*
DMSO
1nM
10nM
100nM
1uM
10uM
Chromomycin A2

Table S1

Antibody	Host Species	kDa	Company	Cat#	Dilution
ERK1/2	R	42/44	Cobb lab	Y691	1:3000
pERK1/2	M	42,44	Cell Signali	9106	1:2000
rpS6-p235/	R	32	Cell Signali	2211	1:1000
rpS6	M	32	Santa Cruz	sc-74459	1:3000
					All 2' Ab is 1:10,000

Name	Gene name	Species	Sequence !	Amplicon	PrimerBank ID or Reference
mUcn3.fwd	Urocortin 3	Mouse	AAGCCTCT	175	21492632a1
mUcn3.rev			GAGGTGCGTTTGGTTGTCATC		
mh18S.fwd	18S	human/mo	GTAACCCG	151	http://www.uic.edu/depts/rrc/cgf/realtime/primerseq.html
mh18S.rev			CCATCCAATCGGTAGTAGCG		
mIns12.fwd	Mouse Insulin I/II	Mouse onl	TGAAGTGC	125/131	PMID: 18669644
mIns12.rev			AGATGCTGGTGCAGCACTGAT		
mPdx1.fwd	Pdx1	Mouse	CCCCAGTT	177	6679269a1
mPdx1.rev			CTCGGTTCCATTCGGGAAAGG		

ID#	Culture time prior to shipping	Age	Sex	Race	BMI	HbA1c	GSIS SI (IID	Viability	Purity
AEAN289	4d	44	Male	White	34.6	5.4%	2.4	95	95
AEBP173		68	Male	White	29.7	5.2%	2.6	95	90